Published in final edited form as:
Cell. 2011 October 28; 147(3): 666–677. doi:10.1016/j.cell.2011.09.046.

Doc2 is a Ca^{2+} sensor required for asynchronous neurotransmitter release

Jun Yao[1], **Jon D. Gaffaney**[1], **Sung E. Kwon**, and **Edwin R. Chapman**[2]
Howard Hughes Medical Institute and Department of Neuroscience, University of Wisconsin, Madison, Wisconsin 53706

SUMMARY

Synaptic transmission involves a fast synchronous phase and a slower asynchronous phase of neurotransmitter release that are regulated by distinct Ca^{2+} sensors. While the Ca^{2+} sensor for rapid exocytosis, synaptotagmin I, has been studied in depth, the sensor for asynchronous release remains unknown. In a screen for neuronal Ca^{2+} sensors that respond to changes in [Ca^{2+}] with markedly slower kinetics than synaptotagmin I, we observed that Doc2, another Ca^{2+}, SNARE, and lipid binding protein, operates on time scales consistent with asynchronous release. Moreover, up- and down-regulation of Doc2 expression levels in hippocampal neurons increased or decreased, respectively, the slow phase of synaptic transmission. Synchronous release, when triggered by single action potentials, was unaffected by manipulation of Doc2, but was enhanced during repetitive stimulation in Doc2 knockdown neurons potentially due to greater vesicle availability. In summary, we propose that Doc2 is a Ca^{2+} sensor that is kinetically tuned to regulate asynchronous neurotransmitter release.

INTRODUCTION

Evoked neurotransmitter release often consists of two kinetically distinct components; one phase in which Ca^{2+} influx triggers rapid synchronous release with a time course of several milliseconds, and another slow asynchronous phase which can last for tens or hundreds of milliseconds at glutamatergic synapses. While fast synchronous release is essential for rapid communication with downstream neurons, asynchronous release allows for the modulation of postsynaptic excitability, on relatively long time scales, which in turn can alter action potential firing patterns (Best and Regehr, 2009; Iremonger and Bains, 2007; Lu and Trussell, 2000; Peters et al., 2010). Moreover, asynchronous release has been implicated in neural network activity, including persistent reverberation (Lau and Bi, 2005).

Fast synchronous release is regulated by the Ca^{2+} sensor, synaptotagmin I (syt I) (Koh and Bellen, 2003). Syt I binds Ca^{2+} ions via its tandem C2 domains, C2A and C2B, with the C2B domain playing a critical role in triggering fusion in response to Ca^{2+} (Mackler et al., 2002; Nishiki and Augustine, 2004a; Robinson et al., 2002; Gaffaney et al., 2008). Syt I triggers fusion via interactions with both SNARE (soluble NSF attachment protein receptor)

[2]Please address correspondence to: Edwin R. Chapman, Ph.D. 1300 University Avenue, 129 SMI, Madison, WI 53706; Telephone: (608) 263-5512; Fax: (608) 265-5512; chapman@physiology.wisc.edu.
[1]These authors contributed equally to the work done in this study.

proteins and membranes (Chapman, 2008). In the absence of syt I, asynchronous release not only persists, but is significantly enhanced (Liu et al., 2009; Nishiki and Augustine, 2004b). A recent study, using photolysis of caged Ca^{2+} to trigger uniform increases in $[Ca^{2+}]_i$ in syt I knockout (KO) hippocampal neurons, revealed that Ca^{2+} signals were transduced to membrane fusion with slower kinetics than in wild-type (wt) cells (Burgalossi et al., 2010). These findings provide direct support for the existence of a yet-to-be identified second sensor with distinct biophysical properties.

A compelling candidate Ca^{2+} sensor for asynchronous release is the double C2 domain protein, Doc2. Three isoforms of Doc2 have been identified: Doc2α, Doc2β, and Doc2γ (Fukuda and Mikoshiba, 2000; Orita et al., 1995; Sakaguchi et al., 1995). All three isoforms are cytosolic proteins consisting of a unique N-terminal sequence and two C2 domains, C2A and C2B. Doc2α and Doc2β bind to phospholipids in response to Ca^{2+} (Kojima et al., 1996; Orita et al., 1995); Doc2γ exhibits less robust Ca^{2+}-dependent membrane binding activity, potentially due to the absence of three acidic Ca^{2+} ligands in the C2A domain of this isoform (Fukuda and Mikoshiba, 2000). Doc2α and Doc2β have both been shown to directly interact with Munc13 and Munc18 and were proposed to modulate secretory vesicle exocytosis at a step that precedes fusion, such as docking or priming (Mochida et al., 1998; Verhage et al., 1997). However, more recent work revealed that the C2 domains of Doc2 not only interact with Ca^{2+} and phospholipids, but can also bind SNARE proteins (Friedrich et al., 2008) and stimulate SNARE-mediated membrane fusion *in vitro* (Groffen et al., 2010).

Doc2α and β modulate secretory vesicle exocytosis in PC12 cells and chromaffin cells (Friedrich et al., 2008; Orita et al., 1996; Sato et al., 2010). These are the predominant isoforms expressed in brain and both are present in presynaptic terminals (Groffen et al., 2006). While Doc2α KO neurons exhibited normal synaptic transmission in response to single action potentials (Sakaguchi et al., 1999), slight defects in short-term synaptic plasticity, long-term potentiation, and memory retention were observed (Sakaguchi et al., 1999). Moreover, two recent studies concluded that Doc2 regulates Ca^{2+}-dependent spontaneous synaptic vesicle (SV) fusion events (Groffen et al., 2010; Pang et al., 2011). Given these earlier findings, Doc2 emerges as a candidate Ca^{2+} sensor that might function to trigger asynchronous exocytosis in neurons.

In the present study, we analyzed Doc2α and Doc2β using *in vitro* time-resolved lipid binding assays and found that Doc2 responds to changes in $[Ca^{2+}]$ with markedly slower kinetics as compared to the cytosolic domain of syt I (syt) and operates on a time scale consistent with asynchronous neurotransmitter release. Via patch clamp recordings of cultured hippocampal neurons, we observed that the extent of asynchronous release can be specifically modulated through knockdown (KD), KO, or over-expression of Doc2. Importantly, syt I-triggered synchronous release was not directly affected by KD/KO of Doc2, but was enhanced during high frequency train stimulation, an effect that is likely due to attenuated competition for vesicles from the asynchronous phase of release. Finally, KD of Doc2α inhibited the occurrence of persistent reverberation in neural networks composed of high density cultures of neurons. Together, these data demonstrate Doc2 is a slow Ca^{2+} sensor that plays a critical role in asynchronous neurotransmitter release.

RESULTS

Doc2 regulates SNARE-dependent fusion *in vitro* via interactions with lipids and SNAREs

If Doc2α or Doc2β serves as Ca^{2+} sensors for SV exocytosis, they would be expected to bind to SNAREs and membranes in a Ca^{2+}-promoted manner. Indeed, previous GST pull-down assays revealed interactions between Doc2β and the target membrane SNAREs (t-SNARE) syntaxin 1A and SNAP-25B (Friedrich et al., 2008; Groffen et al., 2010). We

extended these experiments to study the interaction of Doc2 isoforms with membrane-embedded full-length t-SNAREs using a co-flotation assay; robust Ca^{2+}-promoted binding of both Doc2α and Doc2β was observed (Figures S1A and S1B). We also confirmed that Doc2β (Groffen et al., 2010) as well as Doc2α bound to liposomes harboring phosphatidylserine (PS) in response to Ca^{2+} (Figures S1C and S1D).

We then utilized an established SNARE-mediated membrane fusion assay (Tucker et al., 2004) to assess the abilities of Doc2α and Doc2β to regulate Ca^{2+}-triggered membrane fusion *in vitro*; syt served as a reference. In all three cases, addition of Ca^{2+} triggered an increase in the rate of vesicle fusion. However, under the conditions used in this experiment, Doc2α and Doc2β yielded slower, less efficient fusion than syt (Figure 1A); by titrating Ca^{2+} we also observed conditions under which Doc2β stimulated more robust fusion than syt (e.g. $[Ca^{2+}] < 0.1$ mM). The rank order of Ca^{2+}-sensitivity was Doc2β > Doc2α > syt (Figure 1B; see also (Groffen et al., 2004; Groffen et al., 2006)).

Analogous to syt, the ability of Doc2 to stimulate membrane fusion *in vitro* was strictly dependent on the presence of PS in the vesicles; in all cases, fusion was not observed when PS had been omitted (Figure 1C; left panel) (Bhalla et al., 2005). Interestingly, titration of all three C2 domain proteins revealed that both isoforms of Doc2 were more sensitive to increases in PS, from 15% to 25%, than was syt (Figure 1C; middle and right panels). Thus, the local PS concentration at release sites is likely to have a larger effect on the activity of Doc2 versus syt I *in vivo*.

Under SNARE-free conditions (i.e. using vesicles lacking SNAREs) or in the presence of the cytosolic domain of synaptobrevin 2 (cd-syb), no fusion was observed (Figures S1E–S1G), demonstrating that Doc2α– and Doc2β-regulated fusion reactions are dependent on cognate SNARE pairing.

A hallmark of syt lies in its ability to fold SNAP-25 onto syntaxin, in response to Ca^{2+}, to form functionally active heterodimers (Bhalla et al., 2006), but the 'traditional' fusion assay monitors the fusion of t-SNARE vesicles, containing pre-formed syntaxin•SNAP-25 hetero-dimers, with v-SNARE vesicles (Figure 2A). In order to test whether Doc2 can assemble functional t-SNARE heterodimers, vesicles harboring syntaxin alone were incubated with free SNAP-25 and syt, Doc2α, or Doc2β (Figure 2B). All three C2 domain proteins were able to accelerate fusion between syntaxin vesicles and v-SNARE vesicles in response to Ca^{2+} in the presence of free, soluble, SNAP-25. When SNAP-25 or syt/Doc2 was omitted from the reactions little, if any, fusion was observed. Therefore, analogous to syt, these experiments reveal that Doc2α and β are capable of doing work on SNARE proteins by driving the assembly of functionally active SNARE complexes in response to Ca^{2+} (Figure 2C).

We note that Doc2 efficiently aggregates membranes in response to Ca^{2+} (J.D.G. and E.R.C., unpublished observations), and a recent study demonstrated that aggregation is sufficient to drive membrane fusion *in vitro* using standard fusion assays that employ pre-assembled t-SNARE heterodimers (Hui et al., 2011). However, aggregation cannot drive fusion if 'split' t-SNAREs (i.e. membrane embedded syntaxin plus soluble SNAP-25) are utilized. Hence, the data reported here reveal that Doc2 can regulate fusion in a manner that does not merely involve aggregation of vesicles, but rather requires functional interactions with SNARE proteins.

Doc2 and syt interact with membranes on different time scales in response to changes in [Ca^{2+}]

If Doc2 serves as a Ca^{2+} sensor for asynchronous synaptic transmission, we would predict that it will bind to membranes with slower kinetics, and would disassemble from Ca^{2+}/membrane complexes on much longer time scales than syt, i.e. well after Ca^{2+} microdomains have collapsed in presynaptic boutons. To address this issue, the membrane binding kinetics of syt and Doc2 were determined using a stopped-flow spectrometer. Syt, Doc2α, or Doc2β was rapidly mixed with liposomes - that harbored PS and dansyl phosphatidylethanolamine (dansyl-PE) - plus Ca^{2+}. Fluorescence resonance energy transfer (FRET), from endogenous aromatic residues in each protein to dansyl-PE, resulted in the sensitized emission of the dansyl-acceptor, which was monitored in real-time (Figures 3A and 3B; Figure S2A). The traces were fit with double exponential functions; although a significant fraction of the signal could be attributed to the slow component (30–45% for Doc2, <10% for syt), the fast component predominated and was plotted as a function of liposome concentration (Figure 3C). Doc2α and Doc2β exhibited approximately 4- and 3-fold slower membrane binding kinetics, respectively (Figure 3D). These data suggest that during Ca^{2+} influx, syt will respond first (i.e. before Doc2) to drive rapid exocytosis (Shahrezaei and Delaney, 2005; Burgalossi et al., 2010).

To mimic the rapid decrease in $[Ca^{2+}]_i$ that occurs shortly after influx in nerve terminals, protein•Ca^{2+} • liposome complexes were rapidly mixed with excess EGTA (Figure 3E) and the rates of disassembly were determined at 14°C using vesicles with 25% PS (Figure 3H). The syt data were fitted using single exponential functions, while the Doc2 measurements were fitted using double exponential functions. The slow component of Doc2 disassembly predominated, accounting for ~68–77% of the signal. Doc2α and Doc2β both displayed dramatically slower rates of disassembly (310–320 msec) from vesicles as compared to syt (4.7 msec) (Figures 3F–3H). The rate of disassembly of Doc2 from membranes was dependent on both temperature and the mole fraction of PS in the liposomes. The time constant (τ) was determined for vesicles containing 15% or 25% PS and was plotted as a function of temperature (Figures S2B and S2C). Under all the conditions tested Doc2 disassembly occurred on significantly slower time scales (a few hundred msec) than syt (a few msec).

In summary, these *in vitro* experiments indicate that both isoforms of Doc2 can trigger membrane fusion through interactions with Ca^{2+}, SNAREs, and PS, and support the hypothesis that Doc2 is kinetically tuned to function as a Ca^{2+} sensor for asynchronous neurotransmitter release.

Doc2 knockdown reduces asynchronous release in cultured syt I KO neurons

In the next series of experiments we turned to electrophysiological recordings to determine whether Doc2 acts as a Ca^{2+} sensor for asynchronous neurotransmitter release. We observed significant levels of Doc2α expression in cultured hippocampal neurons (Figure 4A). However, Doc2β was not detected in our cultures by immunoblot analysis using purified Doc2β as a standard (Figure 4B). These findings are consistent with a report indicating that Doc2α is highly expressed in adult neurons (after day 5) whereas Doc2β expression declines during neuronal maturation (Korteweg et al., 2000).

To directly examine the effects of Doc2α on asynchronous release, we first utilized syt I KO neurons, in which the synchronous component of release is largely absent, thus providing a purely asynchronous component of transmission (Geppert et al., 1994; Nishiki and Augustine, 2004b). Cells were infected with lentiviruses encoding short hairpin RNAs (shRNAs) specific for Doc2α or Doc2β, which efficiently knocked down Doc2 expression in

neurons (Doc2α) or HEK-293T cells (Doc2β) (Figures 4A and 4B; Figures S3A and S3B). Comparing evoked excitatory postsynaptic currents (EPSCs) between syt I KO neurons and KO neurons expressing Doc2 shRNAs (Figures 4C and 4D), Doc2β shRNA had no effect on the total charge transfer ($p>0.5$), consistent with the lack of detectable Doc2β protein in these cultures. This lack of an effect by Doc2β shRNA also serves as a negative control; lentiviral infection and expression of a non-relevant shRNA did not influence synaptic transmission in these experiments. Strikingly, we observed a significant decrease in the total charge transfer in Doc2α KD neurons ($p<0.001$). This effect was not due to a reduction in the size of the readily releasable vesicle pool (RRP) or in the number of postsynaptic AMPA receptors, as Doc2α shRNA did not affect either the total postsynaptic current elicited by application of hypertonic sucrose (Figure 4E; $p>0.5$), or the charge transferred during quantal release events (Figures S3C and S3D; $p>0.5$). These findings indicate that Doc2α can modulate asynchronous SV release through a presynaptic mechanism. Furthermore, the impairment of evoked EPSCs by Doc2α shRNA was rescued by lentiviral expression of Doc2β in neurons (Figures 4C and 4D; $p>0.05$). Thus, Doc2β can functionally substitute for Doc2α to drive asynchronous release. The low levels of asynchronous release that persist in Doc2α KD neurons are mediated by residual Doc2 or other, redundant, proteins that also function to regulate asynchronous release.

Next, we investigated the impact of Ca^{2+}-ligand mutations in Doc2 during evoked asynchronous neurotransmitter release. Two Ca^{2+} ligands in C2A and two putative ligands in C2B were neutralized by substituting the native aspartatic acid residues with asparagines (designated as Doc2α-CLM). We first found that over-expression of wt Doc2α in syt I KO neurons led to an increase in charge transfer (Figure 4F and 4G; $p<0.001$). Surprisingly, over-expression of Doc2α-CLM triggered much larger increases in asynchronous release than the wt protein (>4-fold; $p<0.001$). This observation indicates that Doc2α-CLM is a gain-of-function mutant form of Doc2α, which is consistent with previous studies of Ca^{2+}-triggered spontaneous fusion events (Groffen et al., 2010; but see also Pang et al., 2011).

For comparison, we investigated the effects of a loss-of-function alanine mutant form of Doc2β (designated as Doc2β-4A) on asynchronous release in syt I KO neurons (Figure S3E). In this construct, three apolar residues at the distal tips of two presumptive membrane penetration loops (Chapman, 2008) were replaced with alanines (note: the fourth membrane penetration ‘tip’ harbors a naturally occurring alanine). This results in a reduction in side chain volume, thereby reducing the ability of this protein to interact with membranes and stimulate fusion *in vitro* (Groffen et al., 2010). In contrast to wt Doc2β, this mutant form of the protein was unable to enhance asynchronous SV exocytosis (Figure S3F), and thus serves as a negative control.

Finally, we generated a syt I/Doc2α chimera composed of the luminal domain, transmembrane region, and linker of syt I fused to the C2AB domain of Doc2α (TM-Doc2α). In syt I KO neurons, this chimera was targeted to presynaptic boutons, and presumably SVs (Figure S3G), where it resulted in a significant increase in asynchronous glutamate release without affecting the kinetics of the cumulative charge transfer (Figures S3H–J). These experiments demonstrate that the localization of the Ca^{2+} sensor does not account for the kinetic differences between synchronous and asynchronous release reported here.

Doc2 does not affect fast synchronous transmission evoked by single action potentials

The reduction in asynchronous release, due to Doc2α KD, could be the result of a non-specific effect on evoked SV release. In this case, one would expect that changes in synchronous and asynchronous release would be correlated. In order to address this issue we examined wt neurons, which exhibit both phases of transmission (Figure 5A), by first using

AM-EGTA, which slowly chelates intracellular residual Ca^{2+} following action potential triggered Ca^{2+} influx, to virtually abolish asynchronous release (Figures S4A and S4B) (Hjelmstad, 2006; Maximov and Sudhof, 2005; Otsu et al., 2004). Neurons pre-incubated with AM-EGTA, or that expressed Doc2α shRNA, did not exhibit significant changes in EPSC amplitude (Figure 5B). However, the decay kinetics of the EPSCs were markedly faster under both conditions as compared to untreated neurons, resulting in much more rapid cumulative charge transfer during evoked release (Figure 5C; Figures S4E, S4G, S4H, and S4J); the rise time remained unchanged (Figure S4F and S4I). The faster kinetics in Doc2α KD neurons are not caused by changes in postsynaptic AMPA receptors, as the kinetics of individual miniature EPSCs (mEPSCs) were unaffected (Figures S4C and S4D). To quantitatively analyze the fast and slow phases of SV release, the cumulative charge from evoked responses was fit with a double exponential function to determine the amplitude of each component. The charge transferred during the slow asynchronous phase of SV release exhibited a clear reduction in Doc2α KD or AM-EGTA treated neurons (Figure 5D; $p<0.001$); the time constants for asynchronous release were unaffected (Figure 5E; $p>0.05$). We confirmed these results using Doc2α KO neurons (Figures 5H–5M). Importantly, expression of Doc2β in Doc2α KD neurons rescued the observed defects in asynchronous release ($p>0.05$). Furthermore, the fast synchronous component of SV release remained unaffected in Doc2α KD neurons even when Doc2β had been expressed in these cells (Figures 5F and 5G; $p>0.05$). Hence, the effects of Doc2α and Doc2β on SV release are specific for the asynchronous phase of transmission.

Congruent with the effects of over-expression expression of Doc2 in syt I KO neurons (Figures 4F and 4G), up-regulation of either Doc2 isoform in wt neurons resulted in the selective enhancement in the asynchronous phase of SV release (Figure S5). These results further confirm the idea that Doc2 selectively regulates the asynchronous phase of release in wt neurons.

Doc2-triggered asynchronous release competes with fast synchronous release for synaptic vesicles during high frequency train stimulation

Given the notion that during repetitive stimulation, synchronous release might be enhanced when asynchronous release has been attenuated, due to potential competition for the same set of vesicles (Hagler and Goda, 2001; Otsu et al., 2004), we examined synaptic responses evoked by high frequency train stimulation (20 Hz/40 APs) under a variety of conditions (Figure 6A). We first estimated the RRP size by extrapolating the cumulative charge transfer during the train (Liu et al., 2009) and found, consistent with Figure 4E, little change in Doc2α KD neurons (Figure 6B; $p>0.5$). However, we did observe a small but significant reduction in the RRP size in AM-EGTA treated neurons ($p<0.001$), due to impairment of both the asynchronous (Figure 5D) and synchronous phases of release (Figure 5F).

To probe for changes in asynchronous release resulting from Doc2α KD during train stimulation, we calculated the tonic charge as the difference between the total and phasic charge (Groffen et al., 2010; Hagler and Goda, 2001; Otsu et al., 2004), and observed a lower fraction of tonic charge transfer in Doc2α KD treated neurons, as compared to control neurons (Figure 6C). However, even in AM-EGTA treated neurons, we still observed some degree of tonic charge transfer during the train (Figures 6A and 6C). These tonic currents can probably be attributed to accumulation of neurotransmitter in the synaptic cleft and, possibly, to spill-over from neighboring synapses (Hagler and Goda, 2001; Kullmann and Asztely, 1998; Makino and Malinow, 2009; Tong and Jahr, 1994).

To distinguish the tonic current induced by ‘real’ asynchronous presynaptic release from the tonic current caused by glutamate accumulation, we analyzed the cumulative charge transfer kinetics at the beginning of the stimulus train, before glutamate can accumulate in the

synaptic cleft. We found that Doc2 KD and AM-EGTA treated neurons both exhibited slower rates of tonic charge build-up during the early stages of the train (Figure 6D), as compared to control neurons. These results were confirmed by the histograms shown in Figures 6E–6G. Furthermore, and consistent with the data reported above regarding EPSCs triggered by single action potentials, the first EPSC in the train exhibited a much faster decay in Doc2α KD neurons or AM-EGTA treated neurons (Figures 6H and 6I; $p<0.001$), again demonstrating attenuated asynchronous release.

Doc2α KD and AM-EGTA treated neurons exhibited slower rates of synaptic depression, versus control neurons, during repetitive stimulation (Figure 6J). These findings indicate that attenuation of asynchronous release makes more vesicles available for synchronous release, consistent with previous studies (Hagler and Goda, 2001; Otsu et al., 2004). Interestingly, the rate of synaptic depression at the beginning of the train in AM-EGTA treated neurons was similar to control neurons, while depression in Doc2α KD neurons was significantly slower. During short-term synaptic plasticity, residual Ca^{2+} might contribute to SV priming (Thomson, 2000) to increase the number of releasable vesicles. Thus the difference between Doc2α KD and AM-EGTA treated neurons is likely due to the buffering of residual Ca^{2+} by AM-EGTA. However, it remains possible that in Doc2α KD neurons, a third Ca^{2+} sensor might respond to residual Ca^{2+} to drive phasic release. In summary, Doc2α KD reduces the tonic phase of transmission during high frequency stimulation.

We confirmed these KD results by recording from Doc2α KO neurons during train stimulation (Figure S6A). Doc2α KO neurons also exhibited a lower fraction of tonic charge transfer and a slower rate of synaptic depression (Figures S6B and S6C), consistent with our observations using a KD approach.

Doc2-triggered asynchronous release is crucial for persistent reverberatory activity in neural networks

Persistent reverberatory activity has been proposed to be important for learning and memory (Lau and Bi, 2005). Because reverberation can be abolished by AM-EGTA (Lau and Bi, 2005; Volman et al., 2007), it was suggested that asynchronous release underlies this long-lived form of recurrent excitation. So, in the final series of experiments, we sought to determine whether Doc2 plays a role in the induction and maintenance of persistent reverberatory activity in neural networks (Figure 7). To address this question, hippocampal neurons were cultured at a high density to support persistent reverberation (Figure 7A). We found that KD of Doc2α strongly diminished both the occurrence and maintenance of reverberation (Figures 7B–D). Therefore, Doc2-triggered asynchronous release is critical for reverberation in this neural network.

DISCUSSION

Doc2 was initially discovered via efforts to isolate cDNA encoding novel C2 domain harboring proteins (Orita et al., 1995; Sakaguchi et al., 1995). As alluded to in the Introduction, early studies revealed that Doc2 interacts with Munc13 and Munc18, suggesting that it might play a role in vesicle priming or docking (Duncan et al., 1999; Friedrich et al., 2008; Higashio et al., 2008; Mochida et al., 1998; Naito et al., 1997; Orita et al., 1997; Verhage et al., 1997). More recently, loss of Doc2 was shown to result in a decrease in the frequency of Ca^{2+}-dependent spontaneous SV fusion events in neurons (Groffen et al., 2010; Pang et al., 2011).

In the present study, we demonstrate that Doc2 binds Ca^{2+} and PS-bearing membranes more slowly than syt I, and ‘hangs-onto’ membranes for hundreds of msec after removal of free Ca^{2+}, suggesting that this protein might drive SV exocytosis during the slow asynchronous

phase of transmission. Indeed, we demonstrate that in hippocampal neurons, Doc2 specifically determines the extent of asynchronous SV exocytosis. Hence, Doc2 is a Ca^{2+} sensor that is kinetically tuned to regulate the slow component of transmitter release.

Doc2 fulfills the biochemical requirements for asynchronous neurotransmitter release

We have extended the biochemical analysis of Doc2 by probing its interaction with full-length membrane embedded t-SNAREs, which more closely mimics the native environment. The use of full length SNAREs is critical, since removal of even the lone transmembrane domain of syntaxin profoundly affects the biochemical properties of the protein (Lewis et al., 2001). Moreover, we utilized a 'split t-SNARE' assay in which free SNAP-25 is added, in *trans*, to fusion reactions that harbored reconstituted syntaxin and syb-bearing vesicles; under these conditions, SNAREs alone are unable to drive fusion. Analogous to earlier work on syt (Bhalla et al., 2006; Hui et al., 2011), we found that Ca^{2+} • Doc2 drives the assembly of functionally active SNARE complexes, resulting in fusion. Together, these experiments demonstrate that Doc2 not only binds, stoichiometrically, to membrane embedded t-SNAREs, but that Ca^{2+} • Doc2 can also carry out work on SNARE proteins. Moreover, we demonstrate that Doc2 must also bind to PS in order to trigger fusion *in vitro*. This property is also analogous to syt; clearly, PS is a critical effector for both syt and Doc2 (Bhalla et al., 2005).

While it has been suggested that the slow Ca^{2+} sensor might possess a higher Ca^{2+} sensitivity than the fast Ca^{2+} sensor syt I - which we observed for Doc2 (Figure 1B) - modeling studies argue that the forward Ca^{2+} binding rate (Shahrezaei and Delaney, 2005), rather than the steady state affinity, dictate the activation of Ca^{2+} sensors in nerve terminals. Our stopped flow experiments indicated that Doc2 triggers vesicle release in an asynchronous manner because it binds and unbinds to Ca^{2+}/membrane on relatively slow time-scales. By extrapolating the τ values in Figure S2 for the disassembly of Ca^{2+} • Doc2 • membrane complexes with EGTA at 25°C, we observed that the *in vitro* data (Doc2α: ~150 msec and ~207 msec for 15% and 25% PS, respectively; and Doc2β: ~120 msec and ~192 msec for 15% and 25% PS, respectively) are consistent with measurements made in neurons (τ ~175–256 msec for the charge transfer during asynchronous release). In summary, these findings reveal that the kinetic properties of Doc2 fulfill the kinetic requirements for the Ca^{2+} sensor for asynchronous synaptic transmission.

Doc2 is required for asynchronous neurotransmitter release in hippocampal neurons

The finding that slow release persists in syt I KO neurons prompted a "two Ca^{2+} sensor" hypothesis where syt I served as the fast sensor while another Ca^{2+} binding protein served as the slow sensor. While the data reported here indicate that Doc2 serves as a slow Ca^{2+} sensor that mediates asynchronous release, we cannot rule out the possibility that Doc2 acts to enable another sensor. Moreover, the two-sensor model is likely to be an oversimplification. Indeed, recent studies indicate that syt II is a fast Ca^{2+} sensor in the calyx of Held synapses (Sun et al., 2007), whereas otoferlin has been proposed to serve as a Ca^{2+} sensor for exocytosis in cochlear inner hair cells (Johnson and Chapman, 2010; Roux et al., 2006). Moreover, other ferlins are also expressed in neurons where they might mediate excitation-secretion coupling (Galvin et al., 2006). The situation for cortical neurons might be even more complicated. Although syt I also functions as the Ca^{2+} sensor for the fast synchronous release in these neurons, a fraction of syt I KO inhibitory cortical neurons exhibit fast synchronous release that is potentially regulated by syt II. Similarly, it was recently reported that Doc2 does not regulate evoked GABAergic SV release in inhibitory cortical neurons (Pang et al., 2011). However, KD of Doc2 protein was not demonstrated in that study, and while clear conclusions cannot be drawn, it remains possible

that cortical neurons employ additional or redundant Ca^{2+} sensors for asynchronous release such that putative loss of Doc2 has little effect on transmission.

Here, we identified Doc2 as a Ca^{2+} sensor for asynchronous release in excitatory hippocampal neurons, whereas syt VII was recently reported to modulate asynchronous release at the zebrafish neuromuscular junction (Wen et al., 2010). We note that loss of syt VII was reported to have no effect on synaptic transmission in small central synapses (Maximov et al., 2008), so the disparate findings regarding the syt VII KO phenotype in mice and fish might be species specific differences. Nonetheless, an interesting emerging idea is that individual fusion machines might contain mixtures of fast and slow Ca^{2+} sensors, and the type and copy number of each sensor might fine-tune the Ca^{2+} sensitivity (Wang et al., 2005), placement relative to Ca^{2+} channels (Young and Neher, 2009), and kinetics of fusion reactions. Indeed, in syt I KO/Doc2 KD neurons, some degree of release persists and this slow release might be mediated by yet another sensor in mouse hippocampal neurons.

Concluding remarks

By screening for Ca^{2+} binding proteins that respond to changes in Ca^{2+} concentration with slow kinetics, we identified Doc2α and Doc2β as potential Ca^{2+} sensors for asynchronous neurotransmitter release. These findings prompted electrophysiological experiments in which Doc2 expression levels were varied and the impact of these alterations on synaptic transmission determined. Modulation of Doc2α expression selectively alters asynchronous release, while the fast phase triggered by syt I remained unaffected. Doc2α KD/KO induced an enhancement in synchronous release during train stimulation, similar to the observations of others when asynchronous release had been attenuated (Hagler and Goda, 2001; Otsu et al., 2004), presumably due to the greater availability of vesicles for fast release. Importantly, all changes in asynchronous release caused by Doc2α KD could be rescued by expression of Doc2β. Combined with our *in vitro* data, we conclude that Doc2 functions as a Ca^{2+} sensor for slow asynchronous SV exocytosis in hippocampal neurons.

EXPERIMENTAL PROCEDURES

cDNA and shRNA constructs

Vectors (pGEX-4T) encoding the re-coded C2 domains of Doc2α (a.a. 88–400) and Doc2β (a.a. 125–412) were provided by M. Verhage (Amsterdam, Netherlands). cDNA for rat syt I C2AB domain (96–421) was provided by G. Schiavo (London, United Kingdom). cDNA encoding full-length human Doc2α and Doc2β was provided by Y. Takai (Kobe, Japan). Asp Ca^{2+} ligands 181, 183 (in C2A), 342, and 344 (in C2B) were mutated to Asn in Doc2α-CLM. The bacterial expression vector for full-length mouse synaptobrevin 2 (syb) (pTW2) and cDNA for full-length rat syntaxin 1A, and the cytosolic domain of mouse syb (cd-syb; a.a. 1–94) were provided by J.E. Rothman (New Haven, CT). cDNA encoding rat SNAP-25B was provided by M.C. Wilson (Albuquerque, NM). Full-length syntaxin 1A, SNAP-25B, and cd-syb were subcloned into pTrcHis to generate N-terminal His_6 fusion proteins for expression in *E. coli*. A plasmid to generate full-length syntaxin 1A•SNAP-25B heterodimer in *E. coli* was described previously (Chicka et al., 2008).

For over-expression and KD experiments in neurons, a bicistronic lentiviral vector system, pLox Syn-DsRed-Syn-GFP (pLox) was used by substituting either the DsRed or GFP coding sequence with the cDNA for human Doc2α or Doc2β or their corresponding shRNA sequence (Origene Technologies Inc.). The pEGFP vector, encoding mouse Doc2β-GFP fusion protein, was provided by R. Duncan (Edinburgh, Scotland).

Fusion assays and data analysis

Fusion assays were carried out in white-bottom 96 well plates in total reaction volumes of 100 μl using a BioTek Synergy HT plate reader equipped with 460/40 nm excitation and 530/25 nm emission filters. Each reaction contained 4.5 μl of t-SNARE vesicles or protein-free vesicles, 0.5 μl of NBD-rhodamine labeled v-SNARE vesicles, and 0.2 mM EGTA. Syt or Doc2 were added to each reaction as indicated in the figures. Samples were incubated at 37°C for 20 min followed by injection of Ca^{2+} to give a final concentration of 1 mM, unless otherwise indicated; reactions were monitored for an additional 60 minutes. The maximum fluorescence signal was obtained by addition of n-dodecyl β-D-maltoside to each reaction well as described (Bhalla et al., 2005; Tucker et al., 2004). The fusion data were normalized by setting the initial signal - prior to the addition of Ca^{2+} - to 0% and the maximal fluorescence signal obtained using detergent to 100%. Data were plotted and analyzed using Prism 4.0 software (GraphPad).

Stopped-flow rapid mixing experiments

Liposomes composed of 15% PS 25% PE, 55% PC, 5% dansyl-PE or 25% PS, 25% PE, 45% PC, 5% dansyl-PE were rapidly mixed with the tandem C2 domains of syt I, Doc2α, or Doc2β at 14, 22, and 30 °C using and an SX.18MV stopped-flow spectrometer (Applied Photophysics, Surrey, U.K.) as described previously (Hui et al., 2005). For association experiments, twice the indicated amount of liposomes plus 0.2 mM Ca^{2+} in one syringe was rapidly mixed with 4 μM protein to yield final concentrations of 0.1 mM Ca^{2+}, 2 μM protein, and the indicated concentration of liposomes. FRET was monitored by exciting aromatic residues at 280 nm and monitoring the emission of the dansyl acceptor via a 470 nm cut-off filter. For disassembly experiments, 44 nM liposomes, 0.2 mM Ca^{2+}, and 4 μM protein in one syringe were rapidly mixed, 1:1, with 2 mM EGTA. All data points are the average of 3 independent experiments in which at least 5 separate traces were averaged for each experiment.

Mouse strains, cell culture, lentiviral infection and transfection

Syt I KO mice were obtained from Jackson Laboratory (Bar Harbor, ME) and Doc2α KO mice were provided by M. Verhage (Amsterdam, Netherlands) (Groffen et al., 2010). Hippocampal neurons were dissected from newborn mice, and incubated in a digestion solution that contained 0.25% trypsin-EDTA (Mediatech), 20 mM glucose and 25 U/ml DNAse. The tissue was washed using Hank's buffered salt solution plus 5 mM HEPES (Mediatech), 20 mM D-glucose and 10% fetal bovine serum (FBS) (Gibco), mechanically dissociated in culture medium, and plated on poly-D-lysine-coated glass coverslips. Cells were grown in Neurobasal culture medium (Gibco) supplemented with 2% B27 (Gibco) and 2 mM Glutamax (Invitrogen). Cultures were maintained at 37°C in a 5% CO_2-humidified incubator.

Lentiviral particles were generated by co-transfecting HEK-293T cells with virus packaging vectors (vesicular stomatitis virus G glycoprotein and Δ8.9) and the pLox vectors containing either mouse Doc2α/β shRNA or human Doc2α/β. Virus particles were collected by ultracentrifugation at 25,000 rpm in an SW-28 rotor (Beckman) in a final volume of 100 μl. Virus was added to neurons at 5 days *in vitro* (DIV), and these neurons were analyzed at 15–17 DIV. For immunoblot blot analysis using HEK-293T cells, the cells were grown in DMEM plus 10% FBS and transfected with Doc2β–GFP with or Doc2β shRNA using a CalPhos mammalian transfection kit (Clontech).

Electrophysiology

Whole-cell patch clamp recordings were performed in voltage-clamp mode using a MultiClamp 700B amplifier (Molecular Devices). The recording chamber was continuously perfused with a bath solution (128 mM NaCl, 30 mM glucose, 5 mM KCl, 5 mM $CaCl_2$, 1 mM $MgCl_2$, 25 mM HEPES; pH 7.3) via a Warner (Hamden, CT) VC-6 delivery system. 50 μM D-AP5 (NMDA receptor antagonist; Tocris) and 20 μM bicuculline ($GABA_A$ receptor antagonist; Tocris) were applied to isolate AMPA receptor-mediated EPSCs. Patch pipettes were pulled from borosilicate glass and had resistances of 3–5 MΩ when filled with internal pipette solution (130 mM K-gluconate, 1 mM EGTA, 5 mM Na-phosphocreatine, 2 mM Mg-ATP, 0.3 mM Na-GTP, 10 mM HEPES; pH 7.3). The series resistance was typically < 15 MΩ and partially compensated to 60–80%. The membrane potential was held at −70 mV. To record evoked EPSCs, presynaptic neurons were stimulated using a theta stimulating electrode, with a voltage step from 0 V to 20–30 V for 1 millisecond, to trigger an action potential; evoked synaptic release was recorded from the postsynaptic neurons. To test the influence of AM-EGTA (Santa Cruz Biotechnology) on evoked release, neurons were preincubated for 30 min with 25 μM AM-EGTA in the bath solution to allow the diffusion of AM-EGTA into cells. To record mEPSCs, 0.5 μM tetrodotoxin (fast sodium channel blocker; Tocris) was added to the bath solution. Data were acquired using pClamp software (Molecular Devices), sampled at 10 kHz, and filtered at 2 kHz. Off-line data analysis of EPSCs was performed using Clampfit and Igor (WaveMetrics) software. Cumulative plots of the total charge transfer were fitted by a double exponential function, using Igor software, to analyze the fast synchronous and slow asynchronous components of synaptic transmission. A single exponential function was used to fit cumulative charge transfer to analyze the overall kinetics of EPSCs in Figure S4. The rise and decay time of EPSCs were measured using Clampfit software. Experiments were performed at room temperature. Data are presented as the mean ± SEM.

Supplementary Material

Refer to Web version on PubMed Central for supplementary material.

Acknowledgments

We thank the Chapman lab and M.B. Jackson for critical comments. This study was supported by a grant from the National Institutes of Health (MH 61876). J.Y. is supported by an American Heart Association postdoctoral fellowship (11POST5720016). E.R.C. is an Investigator of the Howard Hughes Medical Institute.

References

Best AR, Regehr WG. Inhibitory regulation of electrically coupled neurons in the inferior olive is mediated by asynchronous release of GABA. Neuron. 2009; 62:555–565. [PubMed: 19477156]

Bhalla A, Chicka MC, Tucker WC, Chapman ER. Ca(2+)-synaptotagmin directly regulates t-SNARE function during reconstituted membrane fusion. Nat Struct Mol Biol. 2006; 13:323–330. [PubMed: 16565726]

Bhalla A, Tucker WC, Chapman ER. Synaptotagmin isoforms couple distinct ranges of Ca2+, Ba2+, and Sr2+ concentration to SNARE-mediated membrane fusion. Mol Biol Cell. 2005; 16:4755–4764. [PubMed: 16093350]

Burgalossi A, Jung S, Meyer G, Jockusch WJ, Jahn O, Taschenberger H, O'Connor VM, Nishiki T, Takahashi M, Brose N, et al. SNARE protein recycling by alphaSNAP and betaSNAP supports synaptic vesicle priming. Neuron. 2010; 68:473–487. [PubMed: 21040848]

Chapman ER. How does synaptotagmin trigger neurotransmitter release? Annu Rev Biochem. 2008; 77:615–641. [PubMed: 18275379]

Chicka MC, Hui E, Liu H, Chapman ER. Synaptotagmin arrests the SNARE complex before triggering fast, efficient membrane fusion in response to Ca(2+). Nat Struct Mol Biol. 2008; 15:827–835. [PubMed: 18622390]

Dean C, Liu H, Dunning FM, Chang PY, Jackson MB, Chapman ER. Synaptotagmin-IV modulates synaptic function and long-term potentiation by regulating BDNF release. Nat Neurosci. 2009; 12:767–776. [PubMed: 19448629]

Duncan RR, Betz A, Shipston MJ, Brose N, Chow RH. Transient, phorbol ester-induced DOC2-Munc13 interactions in vivo. J Biol Chem. 1999; 274:27347–27350. [PubMed: 10488064]

Friedrich R, Groffen AJ, Connell E, van Weering JR, Gutman O, Henis YI, Davletov B, Ashery U. DOC2B acts as a calcium switch and enhances vesicle fusion. J Neurosci. 2008; 28:6794–6806. [PubMed: 18596155]

Fukuda M, Mikoshiba K. Doc2gamma, a third isoform of double C2 protein, lacking calcium-dependent phospholipid binding activity. Biochem Biophys Res Commun. 2000; 276:626–632. [PubMed: 11027523]

Gaffaney JD, Dunning FM, Wang Z, Hui E, Chapman ER. Synaptotagmin C2B domain regulates Ca2+-triggered fusion in vitro: critical residues revealed by scanning alanine mutagenesis. J Biol Chem. 2008; 283:31763–31775. [PubMed: 18784080]

Galvin JE, Palamand D, Strider J, Milone M, Pestronk A. The muscle protein dysferlin accumulates in the Alzheimer brain. Acta Neuropathol. 2006; 112:665–671. [PubMed: 17024495]

Geppert M, Goda Y, Hammer RE, Li C, Rosahl TW, Stevens CF, Sudhof TC. Synaptotagmin I: a major Ca2+ sensor for transmitter release at a central synapse. Cell. 1994; 79:717–727. [PubMed: 7954835]

Groffen AJ, Brian EC, Dudok JJ, Kampmeijer J, Toonen RF, Verhage M. Ca(2+)-induced recruitment of the secretory vesicle protein DOC2B to the target membrane. J Biol Chem. 2004; 279:23740–23747. [PubMed: 15033971]

Groffen AJ, Friedrich R, Brian EC, Ashery U, Verhage M. DOC2A and DOC2B are sensors for neuronal activity with unique calcium-dependent and kinetic properties. J Neuroche. 2006; 97:818–833.

Groffen AJ, Martens S, Diez Arazola R, Cornelisse LN, Lozovaya N, de Jong AP, Goriounova NA, Habets RL, Takai Y, Borst JG, et al. Doc2b is a high-affinity Ca2+ sensor for spontaneous neurotransmitter release. Science. 2010; 327:1614–1618. [PubMed: 20150444]

Hagler DJ Jr, Goda Y. Properties of synchronous and asynchronous release during pulse train depression in cultured hippocampal neurons. J Neurophysiol. 2001; 85:2324–2334. [PubMed: 11387379]

Higashio H, Nishimura N, Ishizaki H, Miyoshi J, Orita S, Sakane A, Sasaki T. Doc2 alpha and Munc13-4 regulate Ca(2+) -dependent secretory lysosome exocytosis in mast cells. J Immunol. 2008; 180:4774–4784. [PubMed: 18354201]

Hjelmstad GO. Interactions between asynchronous release and short-term plasticity in the nucleus accumbens slice. J Neurophysiol. 2006; 95:2020–2023. [PubMed: 16338991]

Hui E, Bai J, Wang P, Sugimori M, Llinas RR, Chapman ER. Three distinct kinetic groupings of the synaptotagmin family: candidate sensors for rapid and delayed exocytosis. Proc Natl Acad Sci USA. 2005; 102:5210–5214. [PubMed: 15793006]

Hui E, Gaffaney JD, Wang Z, Johnson CP, Evans CS, Chapman ER. Mechanism and function of synaptotagmin-mediated membrane apposition. Nat Struct Mol Biol. 2011; 18:813–821. [PubMed: 21642967]

Iremonger KJ, Bains JS. Integration of asynchronously released quanta prolongs the postsynaptic spike window. J Neurosci. 2007; 27:6684–6691. [PubMed: 17581955]

Johnson CP, Chapman ER. Otoferlin is a calcium sensor that directly regulates SNARE-mediated membrane fusion. J Cell Biol. 2010; 191:187–197. [PubMed: 20921140]

Koh TW, Bellen HJ. Synaptotagmin I, a Ca2+ sensor for neurotransmitter release. Trends Neurosci. 2003; 26:413–422. [PubMed: 12900172]

Kojima T, Fukuda M, Aruga J, Mikoshiba K. Calcium-dependent phospholipid binding to the C2A domain of a ubiquitous form of double C2 protein (Doc2 beta). J Biochem. 1996; 120:671–676. [PubMed: 8902635]

Korteweg N, Denekamp FA, Verhage M, Burbach JP. Different spatiotemporal expression of DOC2 genes in the developing rat brain argues for an additional, nonsynaptic role of DOC2B in early development. Eur J Neurosci. 2000; 12:165–171. [PubMed: 10651871]

Kullmann DM, Asztely F. Extrasynaptic glutamate spillover in the hippocampus: evidence and implications. Trends Neurosci. 1998; 21:8–14. [PubMed: 9464678]

Lau PM, Bi GQ. Synaptic mechanisms of persistent reverberatory activity in neuronal networks. Proc Natl Acad Sci USA. 2005; 102:10333–10338. [PubMed: 16006530]

Lewis JL, Dong M, Earles CA, Chapman ER. The transmembrane domain of syntaxin 1A is critical for cytoplasmic domain protein-protein interactions. J Biol Chem. 2001; 276:15458–15465. [PubMed: 11278966]

Liu H, Dean C, Arthur CP, Dong M, Chapman ER. Autapses and networks of hippocampal neurons exhibit distinct synaptic transmission phenotypes in the absence of synaptotagmin I. J Neurosci. 2009; 29:7395–7403. [PubMed: 19515907]

Lu T, Trussell LO. Inhibitory transmission mediated by asynchronous transmitter release. Neuron. 2000; 26:683–694. [PubMed: 10896163]

Mackler JM, Drummond JA, Loewen CA, Robinson IM, Reist NE. The C(2)B Ca(2+)-binding motif of synaptotagmin is required for synaptic transmission in vivo. Nature. 2002; 418:340–344. [PubMed: 12110842]

Makino H, Malinow R. AMPA receptor incorporation into synapses during LTP: the role of lateral movement and exocytosis. Neuron. 2009; 64:381–390. [PubMed: 19914186]

Maximov A, Lao Y, Li H, Chen X, Rizo J, Sorensen JB, Sudhof TC. Genetic analysis of synaptotagmin-7 function in synaptic vesicle exocytosis. Proc Natl Acad Sci USA. 2008; 105:3986–3991. [PubMed: 18308933]

Maximov A, Sudhof TC. Autonomous function of synaptotagmin 1 in triggering synchronous release independent of asynchronous release. Neuron. 2005; 48:547–554. [PubMed: 16301172]

Mochida S, Orita S, Sakaguchi G, Sasaki T, Takai Y. Role of the Doc2 alpha-Munc13–1 interaction in the neurotransmitter release process. Proc Natl Acad Sci USA. 1998; 95:11418–11422. [PubMed: 9736751]

Naito A, Orita S, Wanaka A, Sasaki T, Sakaguchi G, Maeda M, Igarashi H, Tohyama M, Takai Y. Molecular cloning of mouse Doc2alpha and distribution of its mRNA in adult mouse brain. Brain Res Mol Brain Res. 1997; 44:198–204. [PubMed: 9073161]

Nishiki T, Augustine GJ. Dual roles of the C2B domain of synaptotagmin I in synchronizing Ca2+-dependent neurotransmitter release. J Neurosci. 2004a; 24:8542–8550. [PubMed: 15456828]

Nishiki T, Augustine GJ. Synaptotagmin I synchronizes transmitter release in mouse hippocampal neurons. J Neurosci. 2004b; 24:6127–6132. [PubMed: 15240804]

Orita S, Naito A, Sakaguchi G, Maeda M, Igarashi H, Sasaki T, Takai Y. Physical and functional interactions of Doc2 and Munc13 in Ca2+-dependent exocytotic machinery. J Biol Chem. 1997; 272:16081–16084. [PubMed: 9195900]

Orita S, Sasaki T, Komuro R, Sakaguchi G, Maeda M, Igarashi H, Takai Y. Doc2 enhances Ca2+-dependent exocytosis from PC12 cells. J Biol Chem. 1996; 271:7257–7260. [PubMed: 8631736]

Orita S, Sasaki T, Naito A, Komuro R, Ohtsuka T, Maeda M, Suzuki H, Igarashi H, Takai Y. Doc2: a novel brain protein having two repeated C2-like domains. Biochem Biophys Res Commu. 1995; 206:439–448.

Otsu Y, Shahrezaei V, Li B, Raymond LA, Delaney KR, Murphy TH. Competition between phasic and asynchronous release for recovered synaptic vesicles at developing hippocampal autaptic synapses. J Neurosci. 2004; 24:420–433. [PubMed: 14724240]

Pang ZP, Bacaj T, Yang X, Zhou P, Xu W, Sudhof TC. Doc2 supports spontaneous synaptic transmission by a Ca(2+)-independent mechanism. Neuron. 2011; 70:244–251. [PubMed: 21521611]

Peters JH, McDougall SJ, Fawley JA, Smith SM, Andresen MC. Primary afferent activation of thermosensitive TRPV1 triggers asynchronous glutamate release at central neurons. Neuron. 2010; 65:657–669. [PubMed: 20223201]

Robinson IM, Ranjan R, Schwarz TL. Synaptotagmins I and IV promote transmitter release independently of Ca(2+) binding in the C(2)A domain. Nature. 2002; 418:336–340. [PubMed: 12110845]

Roux I, Safieddine S, Nouvian R, Grati M, Simmler MC, Bahloul A, Perfettini I, Le Gall M, Rostaing P, Hamard G, et al. Otoferlin, defective in a human deafness form, is essential for exocytosis at the auditory ribbon synapse. Cell. 2006; 127:277–289. [PubMed: 17055430]

Sakaguchi G, Manabe T, Kobayashi K, Orita S, Sasaki T, Naito A, Maeda M, Igarashi H, Katsuura G, Nishioka H, et al. Doc2alpha is an activity-dependent modulator of excitatory synaptic transmission. Eur J Neurosci. 1999; 11:4262–4268. [PubMed: 10594652]

Sakaguchi G, Orita S, Maeda M, Igarashi H, Takai Y. Molecular cloning of an isoform of Doc2 having two C2-like domains. Biochem Biophys Res Commu. 1995; 217:1053–1061.

Sato M, Mori Y, Matsui T, Aoki R, Oya M, Yanagihara Y, Fukuda M, Tsuboi T. Role of the polybasic sequence in the Doc2alpha C2B domain in dense-core vesicle exocytosis in PC12 cells. J Neurochem. 2010; 114:171–181. [PubMed: 20403080]

Shahrezaei V, Delaney KR. Brevity of the Ca2+ microdomain and active zone geometry prevent Ca2+-sensor saturation for neurotransmitter release. J Neurophysiol. 2005; 94:1912–1919. [PubMed: 15888526]

Sun J, Pang ZP, Qin D, Fahim AT, Adachi R, Sudhof TC. A dual-Ca2+-sensor model for neurotransmitter release in a central synapse. Nature. 2007; 450:676–682. [PubMed: 18046404]

Thomson AM. Molecular frequency filters at central synapses. Progress Neurobiol. 2000; 62:159–196.

Tong G, Jahr CE. Multivesicular release from excitatory synapses of cultured hippocampal neurons. Neuron. 1994; 12:51–59. [PubMed: 7507341]

Tucker WC, Weber T, Chapman ER. Reconstitution of Ca2+-regulated membrane fusion by synaptotagmin and SNAREs. Science. 2004; 304:435–438. [PubMed: 15044754]

Verhage M, de Vries KJ, Roshol H, Burbach JP, Gispen WH, Sudhof TC. DOC2 proteins in rat brain: complementary distribution and proposed function as vesicular adapter proteins in early stages of secretion. Neuron. 1997; 18:453–461. [PubMed: 9115738]

Volman V, Gerkin RC, Lau PM, Ben-Jacob E, Bi GQ. Calcium and synaptic dynamics underlying reverberatory activity in neuronal networks. Phys Biol. 2007; 4:91–103. [PubMed: 17664654]

Wang P, Chicka MC, Bhalla A, Richards DA, Chapman ER. Synaptotagmin VII is targeted to secretory organelles in PC12 cells, where it functions as a high-affinity calcium sensor. Mol Cell Biol. 2005; 25:8693–8702. [PubMed: 16166648]

Wen H, Linhoff MW, McGinley MJ, Li GL, Corson GM, Mandel G, Brehm P. Distinct roles for two synaptotagmin isoforms in synchronous and asynchronous transmitter release at zebrafish neuromuscular junction. Proc Natl Acad Sci USA. 2010; 107:13906–13911. [PubMed: 20643933]

Young SM Jr, Neher E. Synaptotagmin has an essential function in synaptic vesicle positioning for synchronous release in addition to its role as a calcium sensor. Neuron. 2009; 63:482–496. [PubMed: 19709630]

HIGHLIGHTS

- Doc2 responds to changes in $[Ca^{2+}]$ with slower kinetics than synaptotagmin I.
- Doc2 specifically modulates the asynchronous phase of neurotransmitter release.
- Changes in Doc2 levels indirectly affect synchronous release.
- Doc2 is required for persistent reverberation in a neural network.

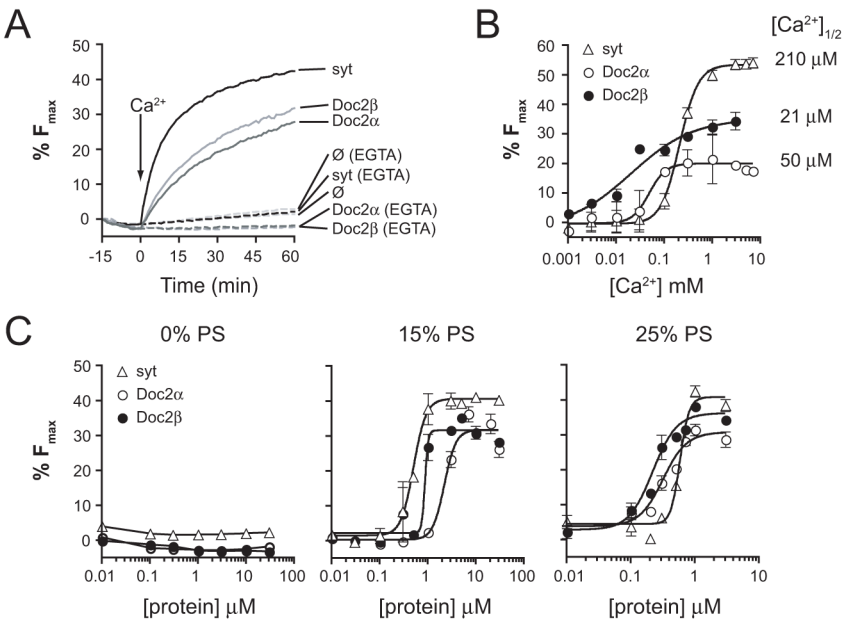

Figure 1.

PS is a critical Doc2α and β effector during regulated membrane fusion. (A) *In vitro* membrane fusion assays were performed in the presence of 3 μM syt, Doc2α, or Doc2β. All three proteins accelerated fusion upon addition of 1 mM Ca^{2+} (arrow). (B) A Ca^{2+} titration for each protein was performed using 15% PS vesicles. Data were fitted with sigmoidal dose-response curves to determine the $[Ca^{2+}]_{1/2}$ values for fusion (inset). (C) Syt or Doc2 titrations were carried out using vesicles with 0, 15 and 25% PS, and data were fit as in panel (B) to calculate EC_{50} values; (0% PS: not applicable; 15% PS: syt, 0.5 μM; Doc2α, 2 μM; Doc2β, 0.9 μM; 25%: syt, 0.6 μM; Doc2α, 0.3 μM; Doc2β, 0.2 μM). Each point represents the mean ± SEM from three independent experiments.

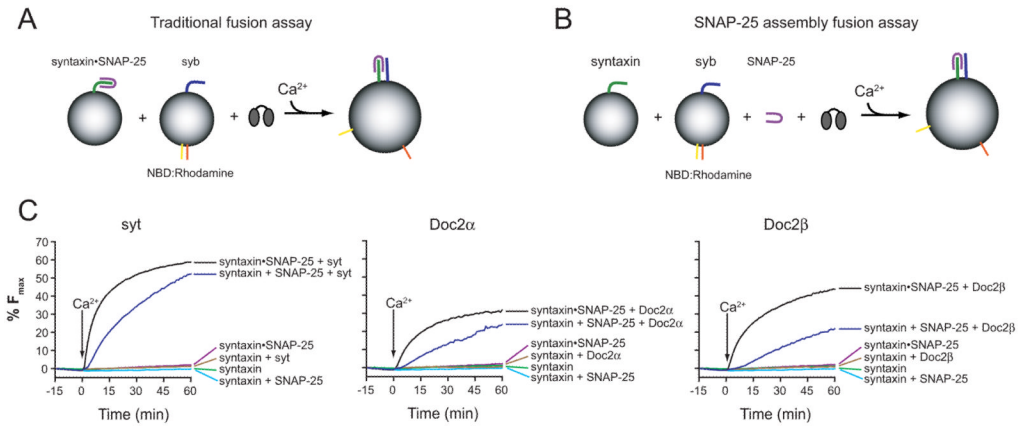

Figure 2.

Doc2α and Doc2β can assemble syntaxin and SNAP-25 into functional SNARE complexes. (A) The 'traditional' fusion assay: vesicles harboring pre-assembled syntaxin•SNAP-25 heterodimers are incubated with syb-harboring vesicles and either syt, Doc2α or Doc2β. (B) Fusion assays were carried out using 'split t-SNAREs' in which syntaxin-alone was reconstituted into the t-SNARE vesicles and free SNAP-25 was subsequently added in a soluble form; under these conditions fusion is not observed unless Ca^{2+} and syt - and, as tested here, Doc2 - are added to drive folding of SNAP-25 onto syntaxin, resulting in fusion activity (Bhalla et al., 2006). (C) Fusion assays using syt (left panel), Doc2α (center panel), or Doc2β (right panel) were carried out with preassembled t-SNARE vesicles or syntaxin vesicles plus free SNAP-25. In the presence of Ca^{2+}, all three proteins were able to drive assembly of active t-SNARE heterodimers capable of fusing with syb vesicles.

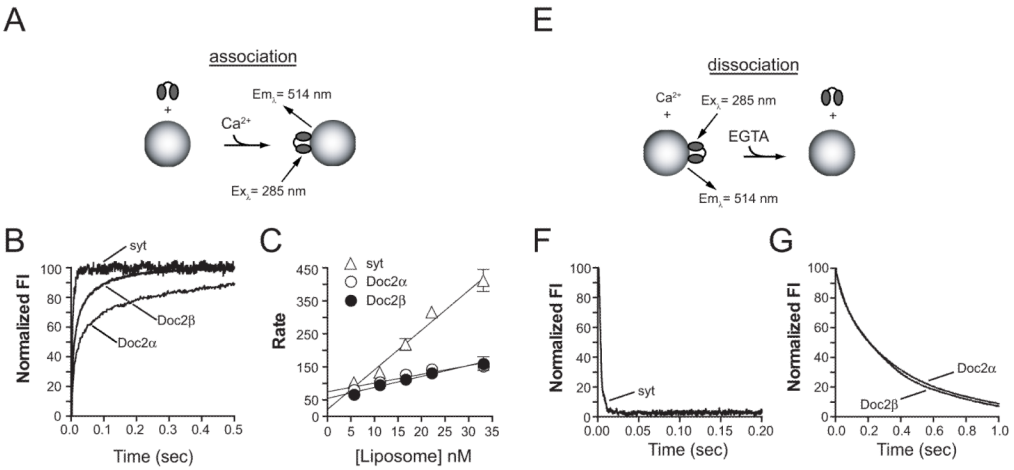

D

protein	k_{on} (10^{10} M^{-1}•sec^{-1})	k_{off} (sec^{-1})	K_d (nM)
syt	11 ± 1	31 ± 20	2.8
Doc2α	2.6 ± 0.4	77 ± 7	30
Doc2β	3.3 ± 0.6	57 ± 10	17

H

protein	k_1,sec^{-1}	Amp 1,%	k_2,sec^{-1}	Amp 2,%	τ, msec
syt	364 ± 30	n/a	n/a	n/a	4.7 ± 0.6
Doc2α	12 ± 1	32 ± 4	2.5 ± 0.4	68 ± 4	320 ± 20
Doc2β	23 ± 4	23 ± 10	3.3 ± 0.5	77 ± 10	310 ± 30

Figure 3.

Doc2 is tuned to respond to changes in [Ca^{2+}] with markedly slower kinetics than syt. Stopped-flow rapid mixing experiments were performed to analyze the kinetics of syt, Doc2α, and Doc2β interactions with vesicles that harbor PS. (A) Association kinetics were monitored via FRET between the endogenous aromatic residues of each protein and a dansyl-PE acceptor in the target vesicles. (B) Representative association traces for each protein showing the first 500 msec (full traces for Doc2α and Doc2β are shown in Figure S2A). (C) Each trace was fit with a double exponential function and the rate of the fast component was plotted as a function of the liposome concentration. Each point represents the mean ± SEM of at least 3 independent experiments. (D) The on-rates, off-rates, and dissociation constants were determined from the plots shown in panel C. (E) Disassembly of Ca^{2+} • Doc2 or syt from liposomes upon rapid mixing with excess EGTA to chelate all Ca^{2+}. (F) The first 200 msec of a representative syt disassembly trace and (G) the first second of representative Doc2α and Doc2β traces are shown. The rate of disassembly was determined for syt by fitting the data with a single exponential function; Doc2 data were fit with a double exponential. (H) The data from at least 5 separate experiments was analyzed and the mean ± SEM for each kinetic component and the τ values were determined.

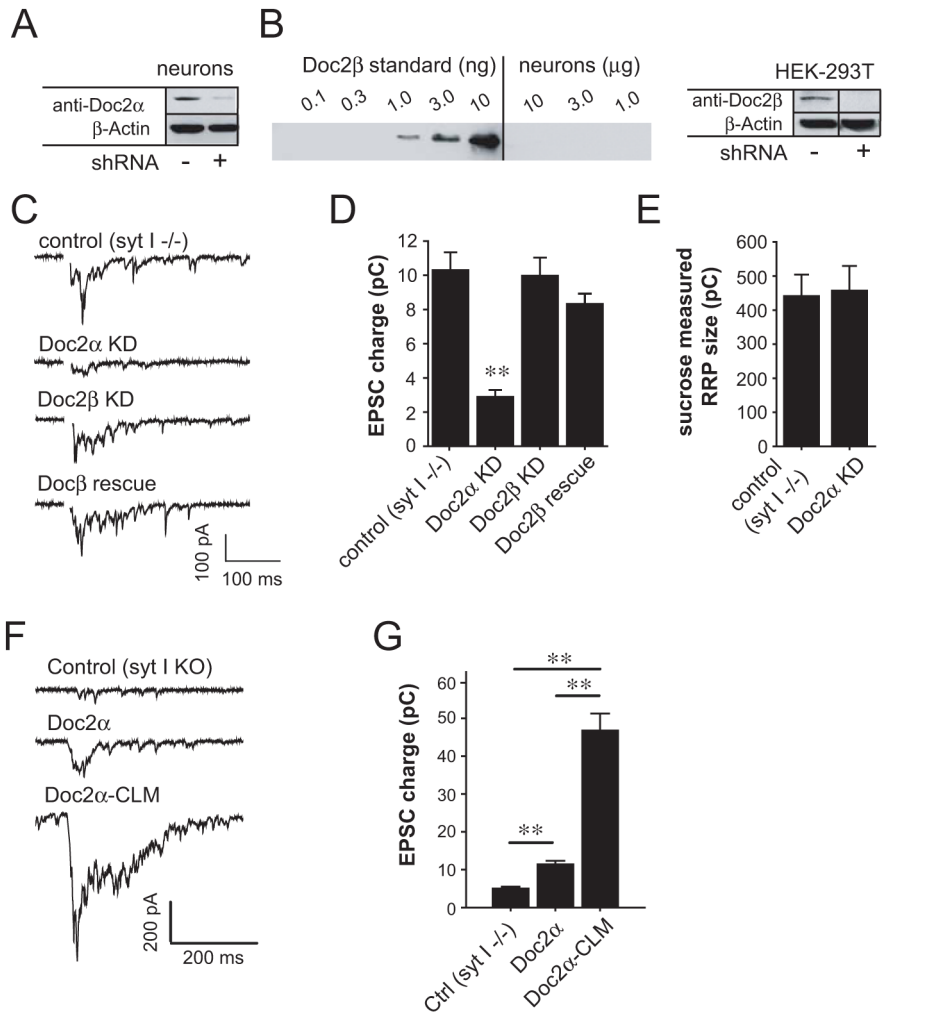

Figure 4.

Doc2α KD reduces asynchronous SV release in syt I knock-out hippocampal neurons. (A and B) Immunoblots of Doc2α (A) or Doc2β (B) in cultured hippocampal neurons. Since Doc2β was not detected (B, left panel), the efficiency of Doc2β shRNA was examined in HEK-293T cells transfected with a Doc2β-GFP construct (B, right panel; vertical line indicates lanes that were removed). Doc2α and Doc2β were reduced ≥ 79% by shRNA KD. (C) Representative traces of evoked EPSCs recorded from syt I KO neurons (control) and lentivirus-infected KO neurons expressing Doc2α shRNA, Doc2β shRNA, or Doc2α shRNA plus Doc2β. (D) Bar graph showing that the total charge transfer over 0.5 s is significantly reduced in the neurons expressing Doc2α shRNA (control, n = 34; shRNA, n = 34), but not Doc2β shRNA (n = 24), or Doc2α shRNA plus Doc2β (n = 23). (E) Averaged total charge of 0.5 M sucrose-induced responses showing little difference between syt I KO neurons (n = 19) and KO neurons expressing Doc2α shRNA (n = 17). (F) Representative EPSC traces from syt I KO neurons, or KO neurons over-expressing wt Doc2α or Doc2α-CLM. (G) Bar graph showing the total charge transfer during EPSCs recorded from syt I KO neurons (n = 33), and KO neurons over-expressing wt Doc2α (n = 16) or Doc2α-CLM (n = 40). ** $p<0.001$. Error bars represent SEM.

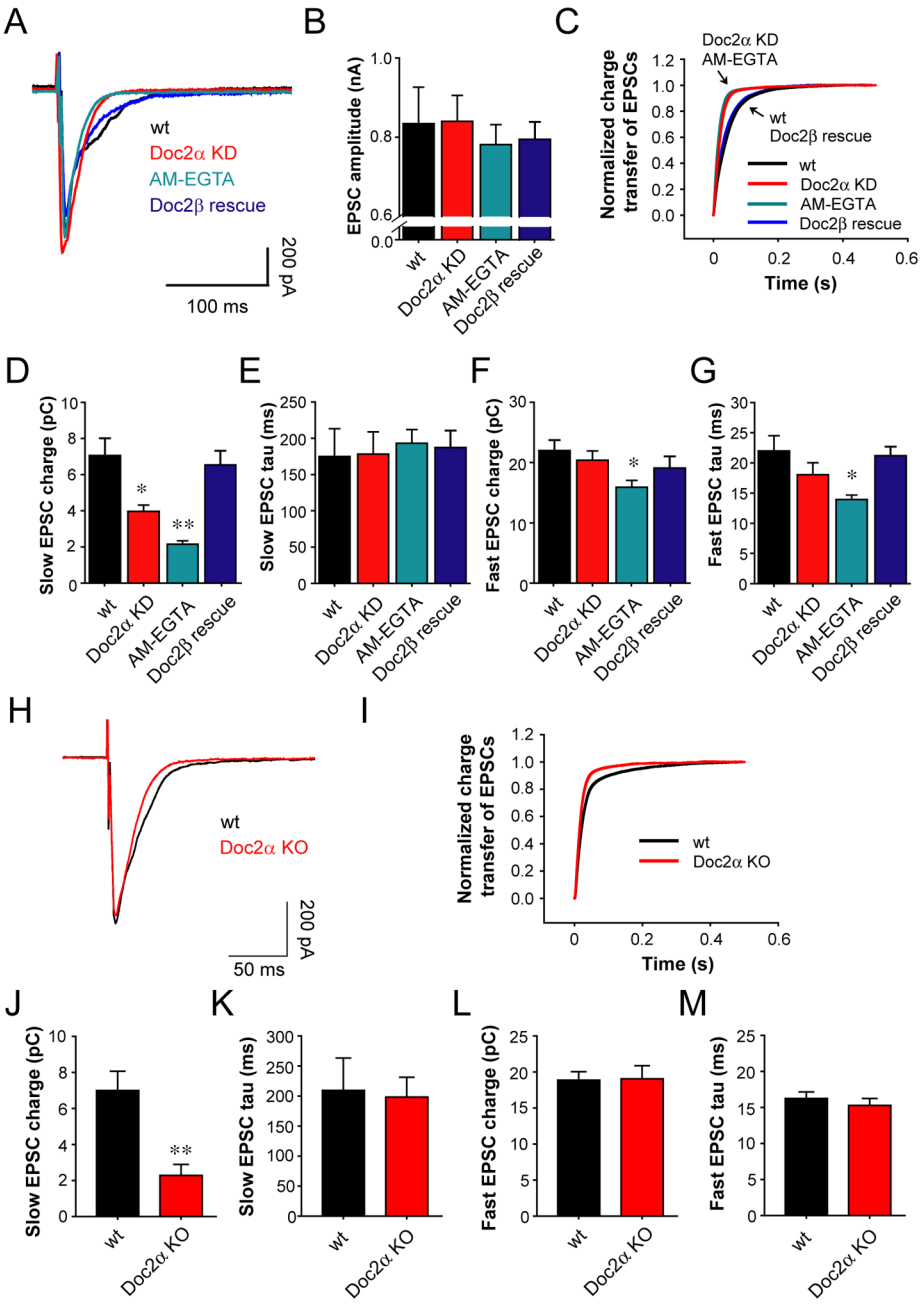

Figure 5.

Doc2α KD specifically reduces the asynchronous phase of SV release in wt hippocampal neurons. (A) Average traces of evoked EPSCs recorded from wt neurons and neurons pre-incubated with 25 μM AM-EGTA, as well as neurons expressing Doc2α shRNA alone or accompanied by expression of Doc2β. (B) Bar graphs summarizing the amplitude of EPSCs recorded from wt neurons (n = 29), neurons treated with AM-EGTA (n = 67), and neurons expressing Doc2α shRNA alone (n = 42) or Doc2α shRNA plus Doc2β (n = 25). (C) Average normalized cumulative EPSC charge transfer over 0.5 s demonstrating that neurons treated with AM-EGTA, or expressing Doc2α shRNA alone, significantly accelerate the decay kinetics of EPSCs, as compared to wt neurons and Doc2α KD neurons expressing Doc2β. (D and E) Bar graphs summarizing the charge (D) and the time constant (E) of the

slow phase of transmission. (F and G) Bar graphs summarizing the charge (F) and the time constant (G) of the fast phase of transmission. (H) Average traces of evoked EPSCs recorded from wt neurons (n = 18) and Doc2α KO hippocampal neurons (n = 23). (I) Average normalized cumulative EPSC charge transfer over 0.5 s from wt neurons and Doc2α KO neurons. (J and K) Bar graphs comparing the charge (J) and the time constant (K) of the slow phase of transmission between wt neurons (n = 18) and Doc2α KO neurons (n = 23). (L and M) Bar graphs summarizing the charge (L) and the time constant (M) of the fast phase of transmission. * $p<0.05$, ** $p<0.001$. Error bars represent SEM.

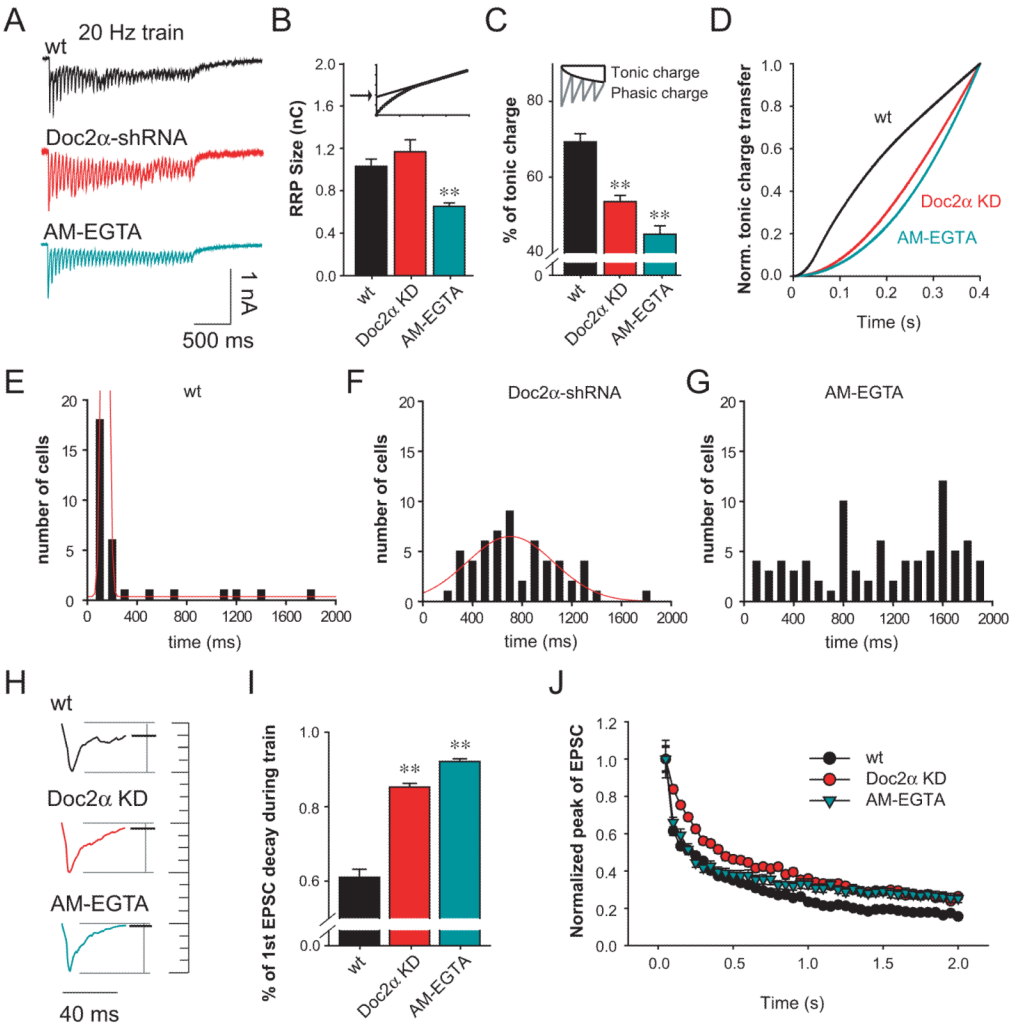

Figure 6.

Doc2α shRNA induces inverse changes in the synchronous and asynchronous components of transmission during high frequency train stimulation. (A) Representative EPSC traces evoked by 40 action potentials at 20 Hz. (B) Bar graph summarizing the RRP size measured by extrapolating the cumulative charge (upper small panel) recorded from wt neurons (n = 33), neurons treated with AM-EGTA (n = 84), or neurons expressing Doc2α shRNA (n = 56). (C) Bar graph showing that neurons treated with AM-EGTA or expressing Doc2α shRNA exhibited significant reductions in the fraction of total tonic charge transfer during the stimulus train. Top panel, diagram showing how the phasic and tonic charge were determined (Otsu et al., 2004). (D) Average normalized cumulative tonic charge transfer over 400 ms demonstrating that AM-EGTA or Doc2α KD significantly decelerated the accumulation of tonic charge. (E-G) Histograms summarizing the build-up of tonic current in wt neurons (E), neurons expressing Doc2α shRNA alone (F), and neurons treated with AM-EGTA (G). The data were fitted with Gaussian curves (red). Doc2α KD induced a left-shift in the distribution, compared to wt neurons and Doc2β rescued neurons. AM-EGTA neurons exhibited a disperse distribution and were not fitted. (H) Typical traces of the first EPSCs during the train showing the extent of decay prior to the next stimulation. The amplitudes were normalized for comparison. (I) Bar graph showing that both Doc2α KD and AM-EGTA treatment induce faster EPSC decay rates. (J) Doc2α KD induced slower

depression of EPSC amplitudes at the beginning of the train compared to control neurons; AM-EGTA treatment gave rise to the same decrease in depression as Doc2α KD during the late stage of the train. ** $p<0.001$. Error bars represent SEM.

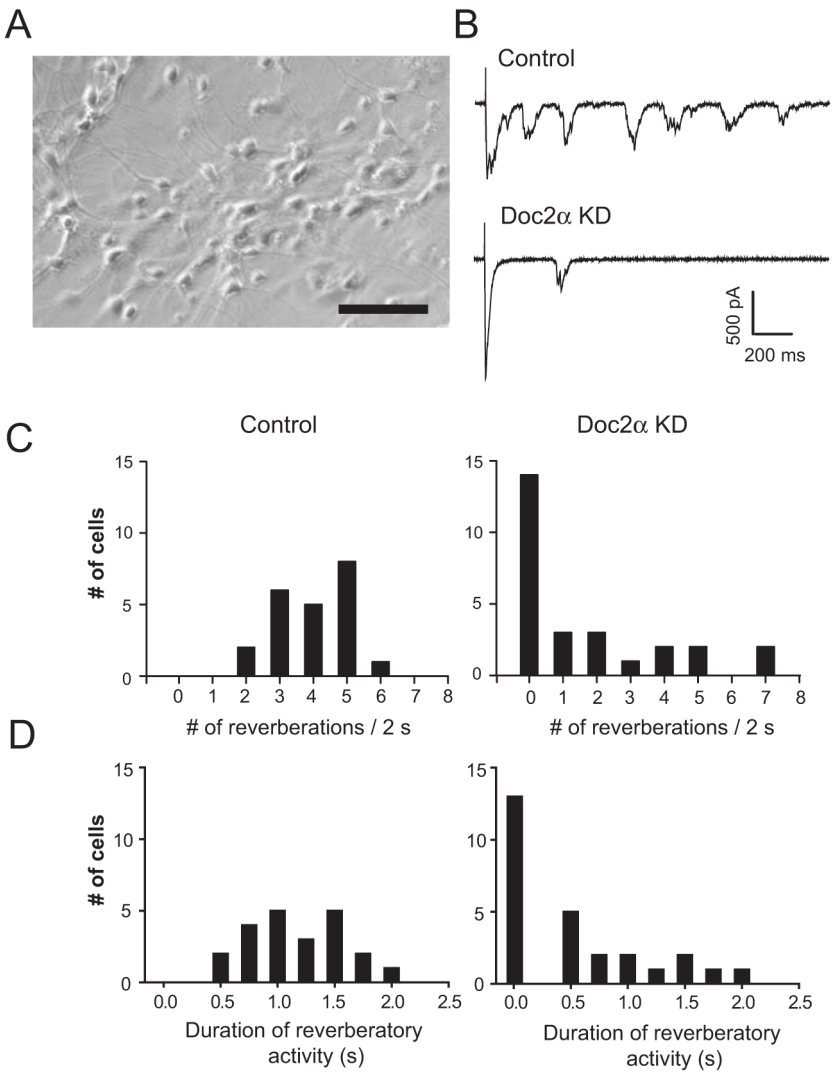

Figure 7.

Doc2α KD reduces evoked reverberatory activity in high density cultures of hippocampal neurons. (A) Sample image of a high density hippocampal culture used to generate reverberatory activity. Scale bar, 100 μm. (B) Representative traces of evoked reverberation recorded from wt neurons (control) and neurons expressing Doc2α shRNA. (C and D) Histograms summarizing the number of reverberatory EPSCs that occurred within 2 s (C) and the duration of the reverberatory activity (D) in wt control (n = 22; left panels) and Doc2α KD neurons (n = 27; right panels).